

**THERMAL EXPANSION AND ISOTOPIC COMPOSITION EFFECTS ON LATTICE  
THERMAL CONDUCTIVITIES OF CRYSTALLINE SILICON**

**Yunfei Chen, Guodong Wang**  
Department of Mechanical  
Engineering and China  
Education Council Key  
Laboratory of MEMS, Southeast  
University, Nanjing, 210096, P. R.  
of China

**Deyu Li**  
Department of  
Mechanical Engineering,  
Vanderbilt University,  
Nashville TN, 37235-1592

**Jennifer R. Lukes**  
Department of Mechanical  
Engineering and Applied  
Mechanics, University of  
Pennsylvania, Philadelphia PA  
19104-6315

**ABSTRACT**

Equilibrium molecular dynamics simulation is used to calculate lattice thermal conductivities of crystal silicon in the temperature range from 400K to 1600K. Simulation results confirmed that thermal expansion, which resulted in the increase of the lattice parameter, caused the decrease of the lattice thermal conductivity. The simulated results proved that thermal expansion imposed another type resistance on phonon transport in crystal materials. Isotopic and vacancy effects on lattice thermal conductivity are also investigated and compared with the prediction from the modified Debye Callaway model. It is demonstrated in the MD simulation results that the isotopic effect on lattice thermal conductivity is little in the temperature range from 400K to 1600K for isotopic concentration below 1%, which implies the isotopic scattering on phonon due to mass difference can be neglected over the room temperature. The remove of atoms from the crystal matrix caused mass difference and elastic strain between the void and the neighbor atoms, which resulted in vacancy scattering on phonons. Simulation results demonstrated this mechanism is stronger than that caused by isotopic scattering on phonons due to mass difference. A good agreement is obtained between the MD simulation results of silicon crystal with vacancy defects and the data predicted from the modified Debye Callaway model. This conclusion is helpful to demonstrate the validity of Klemens' Rayleigh model for impurity scattering on phonons.

**INTRODUCTION**

Silicon is a fundamental material for semiconductor industry. The thermal conductivity of silicon is a key parameter for the design of the electronic device. With the rapid growth of the microprocessor running speed, the removal of the Joule heat becomes critical for the next generation of electronic

devices. With the ready availability of isotopically purified source materials, the isotope effect has undergone reexamination over the last decade. Isotopically purified diamond [1–3] displays a room-temperature isotope effect on the order of 40% at room temperature. In a very thorough investigation of the isotope effect in germanium, Asen-Palmer et al.[4] showed that an isotopically purified sample had thermal conductivity 30% larger compared to natural abundance Ge. Ruf et al in their series papers [5,6] reported the maximum thermal conductivity of highly enriched (99.8588%) <sup>28</sup>Si silicon is six times larger than that in nature silicon around 20K. At room temperature, a thermal conductivity of enhancement of 60% compared with nature silicon is measured. However, Kremer et al [7] remeasured isotopically enriched <sup>28</sup>Si (enrichment better than 99.9%) in temperature range 5-300K. Their measured *k* of isotopically enriched <sup>28</sup>Si exceeds that of nature Si by  $10 \pm 2\%$  at room temperature, which is in disagreement with the early Ruf's measurement. In fact the enhancement of 60% in thermal conductivity for isotopically enriched <sup>28</sup>Si cannot be reconciled with theoretical predictions [8-13], which gave at most, a 20% increase. Isotopic effects on lattice thermal conductivity can be explained by the mass difference from Klemens formula [10]. The Rayleigh scattering rate depends on the mass difference and the strain fields among the impurity atoms and the host matrixes. However, this simple formula only accounts for at most a few percent effects on thermal resistance resulted from single isotope-phonon scattering process for diamond material [3,14,15] at below room temperatures. Murakawa et al [16] used EMD method to discuss the isotope composition effects on lattice thermal conductivity of Si and Ge. The results of calculation showed

that thermal conductivity of mixed isotope-silicon is smaller than that of pure isotope silicon. The results also showed that a pure isotope with a light mass has a large thermal conductivity.

At higher temperatures, Umklapp scattering processes will dominate in phonon scattering processes. Above the Debye temperature, the lifetime of three-phonon scattering process is inversely proportional to temperature while the specific heat and phonon group velocity are temperature independent. The relation between the thermal conductivity and temperature can be approximated as  $k \propto T^{-1}$  in according with the kinetic theory. In practice, the behavior of  $k \propto T^{-1}$  is actually observed at some fraction of the Debye temperature, for example at 1/4 of Debye temperature for argon [17] and at 1/10 of Debye temperature for silicon. However, experimental work on unconstrained argon samples [18] revealed a quadratic temperature term in addition to the theoretically predicted inverse temperature dependence. The authors attributed this extra term to higher order four phonon interactions. G.A. Slack [19] carried out experimental work on crystal silicon. He also demonstrated that the phonon or lattice thermal conductivity decreases faster than  $1/T$  at high temperature. As the temperature exceeds Debye temperature  $\theta$ , the four phonon processes should be taken into account in the simple Callaway model. When the temperature is over  $1.6\theta$ , the electronic thermal conductivity is found and it should not be neglected. However, it should be caution that thermal expansion also contributes to thermal resistance. With the increase of the temperature, lattice constant for silicon increases in Table 1. As pointed out by Dugdale and MacDonald [20] that the differential lattice expansion in the presence of a temperature gradient, for example, the relative expansion of hotter regions and compression of cooler regions for materials with a positive thermal expansion coefficient, creates another source of momentum transfer that further reduces thermal conductivity beyond that determined by three-phonon processes alone. Using the kinetic theory of phonon gases, they linked thermal conductivity to thermal expansion by defining the phonon mean free path as the inverse product of thermal expansion coefficient and temperature. Christen and Pollack [18] whose experimental work agrees well with the first principle calculations on the contribution of the anharmonic crystal force to thermal resistance, also attributed the deviation from  $1/T$  behavior to the effects of thermal expansion on the lattice vibrational frequencies.

So far, a large number works have been carried out on molecular simulation of lattice thermal conductivities for crystal silicon,  $\text{Si}_3\text{N}_4$  and crystal argon [21-25]. However, most previous work concentrated on discussing the validity of the MD simulation results at particular temperature. They seldom investigated lattice thermal conductivity over a large temperature range. In fact, it is more important to explore the temperature dependence of the lattice thermal conductivity over a large temperature range in order to find the N and U

scattering mechanism. In this paper, equilibrium molecular dynamics (EMD) is employed to simulate lattice thermal conductivity of crystal silicon with different isotopic and vacancy compositions. The Klemens' Rayleigh model is used to account for impurity-phonon scattering rates. The direct calculated thermal conductivity from the modified Debye Callaway model integrated with the Klemens' Rayleigh model agreed well with the MD simulation data. Furthermore, the MD simulation result confirmed that for the same defect concentration, the phonon-vacancy scattering rate is stronger than that caused by the isotopic atoms due to only mass difference. Thermal expansion provides another channel for thermal resistance.

### 1. Green-Kubo method

In molecular dynamics simulation methods, there are two widely used ways to calculate the lattice thermal conductivity. One method, nonequilibrium molecular dynamics (NEMD), relies on imposing temperature gradients across the simulation cell and calculates the thermal conductivity directly from Fourier's law. By contrast, the Green-Kubo approach is an EMD method that uses current fluctuations to compute the thermal conductivity via the fluctuation-dissipation theorem. A large number previous works [22,23,24] have compared their advantages and disadvantages. In general, NEMD converges faster and saves computation time. The problem is that larger temperature gradient has to be imposed in the simulation cell, which caused the doubt on the feasibility of Fourier's law. Finite size effect is another drawback for this method due to the boundary scattering at the two ends with fixed temperature conditions in NEMD. In order to remove the finite size effects on the simulation results, linear fitting procedure is proposed in Schelling's work [25]. This requires many set calculations, which results in the similar computation burden compared with the Green-Kubo method. In this paper, the Green-Kubo EMD method is used to calculate thermal conductivities of crystal silicon. Stillinger-Weber(SW) potential [26] is employed to describe diamond structure of crystal silicon. The interaction forces among atoms and the thermal current can be calculated from the SW potentials. Once the thermal current obtained, the lattice thermal conductivity can be expressed through the equilibrium current-current autocorrelation function according to the Green-Kubo theory. Quantum corrections are also introduced in this paper to take into account for the different quantum occupation of phonon states from the classical Boltzmann distribution, particularly for simulated temperature below Debye temperature. In order to compare simulation results with the experimental data directly, it is assumed that the mean kinetic energy of the simulated system equals that of the corresponding quantum system at temperature  $T$  including the zero point energy. More details about the simulation process can be referred to Volz and Schelling's work [21, 25].

#### 1.1. Finite size effects

It is an intrinsic characteristic that finite size affects simulated results for MD. For NEMD, the finite size effect is caused by the phonon scattering on the heat source and heat

sink due to the simulation domain size less than the phonon mean free path in an infinite system. In this case, it is predicted that the finite size effect limits the simulated data, i.e. with the increase of the simulation cell size, the simulated result will increase. In EMD, the size artifacts may be caused by the cutoff frequency and the periodic boundary conditions. In the case with periodic boundary conditions, a phonon may pass the same point in space several times without scattering. Since the system may retain some dynamical information during the passage of the phonon, artificial correlations may exist in the autocorrelation function. In this case, the correlation function may not be reliable for time longer than the time required for passage of the phonon across the simulation cell. With the change of simulation cell size, the final simulation results are different. Table 2 listed the final simulation data for cases with difference size scales. It can be found the simulation results tend to stable as the atom number exceeds 512. Furthermore, in order to decrease the finite size effects, the averaged thermal conductivity calculated from several runs with different random generators is set as the final data in this paper.

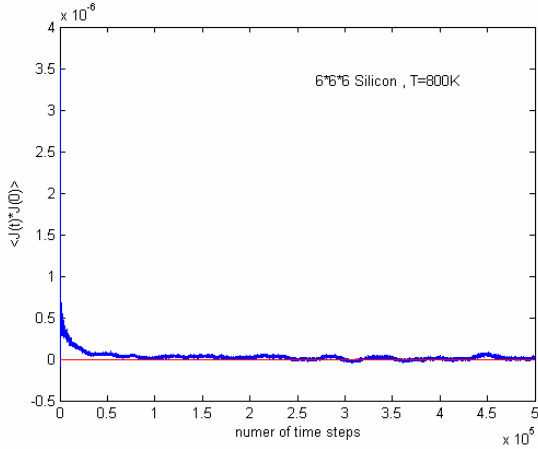


Fig.1. Current-current correlation function

### 1.2. Heat current autocorrelation decay

In the simulation process, time step and total time step number affected the computation time and the reliability of the final results directly. If the time step is set too smaller, it takes long computation time for the system to reach equilibrium state. In this paper, the time step is set as  $dt = 0.5745 fs$ . Total simulation time is about 3ns. In this case, total time step number is about 5 million for the autocorrelation function of heat flux convergence to zero. Even so, it is still a difficult task for the autocorrelation function of heat flux convergence to zero completely at low temperatures. Specially, for temperature below 900K, the autocorrelation function of heat flux will oscillate up and down along the horizontal axis shown as Fig.1. Fig.1 presents the relationship between the autocorrelation function of heat flux versus the time. In this case, the final simulation results depend on the integration time step. To cancel such dependence and save computation time, the results for the current-current autocorrelation function are fit to an exponential function of  $\tau$ , which is then integrated [21,22,23].

In this paper, this method is used to dispose the final data as temperature is below 900K. As temperature is over 900K, the autocorrelation functions of heat flux in formula can be calculated by direct integration method [25].

$$k_{MD} = \frac{\Delta t}{3k_B T^2 V} \sum_{m=1}^M \frac{1}{N-m} \sum_{n=1}^{N-m} J_\mu(m+n) J_\nu(n) \quad (1)$$

Where  $N$  is the total time step in the simulation process and  $M$  is the integration time step. In order to get the data as precise as possible, the total time step should be long enough to guarantee that the heat current-current autocorrelation function converges to zero. For materials with large thermal conductivity such as crystal silicon, the total time step should be as larger as 3 millions.

### 2. Modified Debye Callaway model

In 1958, Callaway [11] proposed a phenomenological model to describe the lattice thermal conductivity of crystal structures at low temperature. The model assumes a Debye-like phonon spectrum with no anisotropies or particular structures in the phonon density of states, i.e., no distinction of polarization between longitudinal and transverse phonons and one averaged sound velocity. The relaxation time scales of the phonons are all frequency and temperature dependant. A correction term is introduced in this model to counteract the effect of treating the phonon N scattering processes as entirely resistive processes. However, the correction term is usually neglected due to its small value for materials with point defects or impurities. Holland [12] extended the Callaway theory to include explicitly the thermal conductivity by both transverse and longitudinal phonons. The variation of the phonon relaxation times with frequency and temperature strongly depend on the actual phonon branches and its dispersions are considered separately. The drawback of Holland's model is that it neglects the correction term in the Callaway's theory. For pure or highly enriched isotopic crystal diamond [3], it has been proved that neglecting the correction term causes misunderstanding of the theoretic predicted results compared with the experimental data. In this case, it is the Normal scattering processes rather than the U scattering or impurity scattering processes dominate in phonon transport at the temperature around the maximum thermal conductivity. The N scattering processes determine the phonon mean free path. In this paper, the modified Debye Callaway model is used to predict the lattice thermal conductivity of crystal silicon. Following Callaway theory, the thermal conductivity can be written as [9]

$$k = k_1 + k_2 \quad (2)$$

$k_2$  in formula (2) is the correction term that accounts for the unresistive nature of N scattering processes. In Holland's model,  $k_1$  was separated into LA and TA contributions  $k_T, k_L$ .

$$k_1 = k_1^T + k_1^L \quad (3)$$

Those terms in formula (3) are defined as

$$k_1^T = \frac{2}{3} H_T T^3 \int_0^{\theta_1/T} \tau_C^T(x) J(x) dx \quad (4)$$

$$k_1^L = \frac{1}{3} H_L T^3 \int_0^{\theta_2/T} \tau_C^L(x) J(x) dx \quad (5)$$

where

$$\tau_C^T(x) = (\tau_{TN}^{-1} + \tau_{TR}^{-1})^{-1} = (\tau_B^{-1} + \tau_i^{-1} + \tau_{TN}^{-1} + \tau_{TU}^{-1})^{-1} \quad (6)$$

$\theta_1, \theta_2$  are the specified temperatures in silicon dispersion relations, which are listed in Table 3.

$$\tau_C^L(x) = (\tau_{LN}^{-1} + \tau_{LR}^{-1})^{-1} = (\tau_B^{-1} + \tau_i^{-1} + \tau_{LN}^{-1} + \tau_{LU}^{-1})^{-1} \quad (7)$$

$$J(x) = \frac{x^4 e^x}{(e^x - 1)^2} \quad (8)$$

$$x = \frac{\hbar\omega}{k_B T}; \quad H_j = \frac{k_B}{2\pi^2 v_j} \left(\frac{k_B}{\hbar}\right)^3; \quad j = T, L \quad (9)$$

In the modified Debye Callaway model, the  $k_2$  term is given in the same formula as that in Callaway theory.

$$k_2 = k_2^T + k_2^L \quad (10)$$

$$k_2^T = \frac{2}{3} H_T T^3 \frac{\left[ \int_0^{\theta_1/T} \frac{\tau_C^T(x)}{\tau_{TN}(x)} J(x) dx \right]^2}{\int_0^{\theta_1/T} \frac{\tau_C^T(x)}{\tau_{TN}(x)\tau_{TR}(x)} J(x) dx} \quad (11)$$

$$k_2^L = \frac{2}{3} H_L T^3 \frac{\left[ \int_0^{\theta_2/T} \frac{\tau_C^L(x)}{\tau_{TL}(x)} J(x) dx \right]^2}{\int_0^{\theta_2/T} \frac{\tau_C^L(x)}{\tau_{TL}(x)\tau_{LR}(x)} J(x) dx} \quad (12)$$

As shown in Table 3, it needs 4 parameters to determine thermal conductivities from formula (2). Those parameters are  $B_{TN}, B_{LN}, B_{TU}, B_{LU}$ , which are used to describe the phonon N and U scattering process. The coefficient  $A_i$  is used to calculate the phonon isotopic scattering time scale. According to the Klemens model, it can be evaluated as

$$\tau_i^{-1} = \tau_{\delta M}^{-1} + \tau_{\delta R}^{-1} = (A_{\delta M} + A_{\delta R})\omega^4 = A_i\omega^4 \quad (13)$$

Where  $\tau_{\delta M}^{-1}$  is the relaxation rate of phonon scattering on point defects due to mass difference.  $\tau_{\delta R}^{-1}$  is the relaxation time due to the relative displacements of neighboring atoms.

$$A_{\delta M} = \frac{nV}{4\pi v_s^3} \left(\frac{\delta M}{M}\right)^2 \quad (14)$$

The volumetric concentration of the point imperfections and the mass and crystal volume of the host atom are  $n, M$  and  $V$ , respectively. The mass difference introduced by the imperfection compared to the host atom is  $\delta M$ . The average

velocity of sound  $v_s$  is approximated by longitudinal and transverse phonon velocities at low frequency, i.e.

$$v_s^{-1} = \frac{1}{3}(v_L^{-1} + 2v_T^{-1}) \quad (15)$$

The insertion of impurity atoms or point defects induces elastic strain in the lattice. This leads to the changes of the phonon velocities and/or wavevectors. The scattering rate  $\tau_{\delta R}^{-1}$  is given by

$$\tau_{\delta R}^{-1} = A_{\delta R}\omega^4 \quad A_{\delta R} = \frac{2nV}{\pi v_s^3} Q_0^2 \gamma^2 \left(\frac{\delta R}{R}\right)^2 \quad (16)$$

Where  $\gamma$  is the Gruneisen constant. Typical values  $Q_0$  [27] reported for  $K^+$  impurities in NaCl and vacancies in KCl are listed in Table 3.

**Table 1, Lattice parameters at different temperature**

T (K)	Lattice constant (nm)	T (K)	Lattice constant (nm)
300	0.5431092	900	0.5443130
400	0.5432677	1000	0.5445423
500	0.5434537	1100	0.5447754
600	0.5436557	1200	0.5450121
700	0.5438685	1300	0.5452514
800	0.5440882		

### 3. Simulation results and Discussions

Thermal expansion is considered in this paper to account for its effect on lattice thermal conductivities. In most previous MD works [21,25], the lattice constant is disposed as a fixed constant at different temperatures. However, in fact, thermal expansion results in the increase of lattice constant with the increase of temperature. The lattice parameter at  $a(T)$  is given by

$$a(T) = a_0 \left( \int_{295.7}^T \alpha(T) dT + 1 \right) \quad (17)$$

where  $a_0$  is the lattice parameter at 295.7 K.  $\alpha(T)$  is the linear thermal expansion coefficients. The lattice parameters can be evaluated from formula (17) for different temperatures. Its values are listed in Table 1.

Two lattice parameter cases are introduced in this paper. The first does not consider thermal expansion effects on lattice constant and a fixed lattice constant at temperature 295.7 K is used in the whole simulation temperature range 400~1600K. The second uses the experimentally determined temperature dependent lattice parameters listed in Table 1. Fig.2 gives the lattice thermal conductivities from the two cases. As expected, the value calculated from the temperature dependent lattice parameter case is smaller than that from the fixed parameter case. This proved that thermal expansion created another type of thermal resistance for phonon transport. In Fig.2, the fitted curve is calculated from the modified Debye Callaway model. The parameters are listed in Table 3. For pure crystal silicon,

the impurity scattering time  $\tau_i^{-1}$  in formula (6) is set as zero. It can be found in Fig.2 that the fitted curve agrees well with the simulated data from the temperature dependent lattice parameter case as temperature is over 800K. When the temperature is below 800K, the simulated data is higher than the fitted value from the modified Debye Callaway model. This is caused by the molecular dynamics itself. As temperature is below 800K, it takes long time for the current-current correlation function decay to zero, which results in the increase of the statistical error. Experimental data from Slack's result [19] are also depicted in Fig.2 shown as solid circles. In the whole temperature range from 400K to 1600K, the simulated data is higher than the experimental data. Previous work [21,28] assumed that the lattice of MD is perfect. The lattice thermal conductivity of perfect crystal may be higher than the experimental data, in which samples are certainly contained some defects. However, a caution point should be pointed out that this could be also caused by the parameter of S-W potential. Another reason is due to the statistical error in the simulation process. The error bar was not depicted in Fig.2 in order to give clear view. Anyway, the error is about 10~15% as depicted in Fig.3 for the simulated data at temperature below 800K.

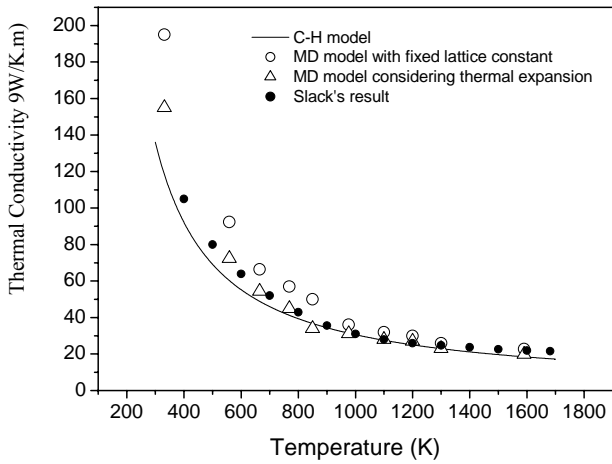


Fig.2. Lattice thermal conductivities of pure silicon simulated by MD, evaluated from the modified Debye Callaway model, and measured experimentally [19]

Isotopic effects on lattice thermal conductivity can be estimated from the modified Debye Callaway model from formula (2). In formula (13), the isotopic scattering rate coefficients due to mass difference can be calculated, which is about  $A_{\delta M} = 4.259 * 10^{-48}$  for  $n=0.05787\%$   $^{29}\text{Si}$ . The isotopic atom radius is estimated equal to the radius of the host atoms. So the scattering due to the elastic strain is neglected.  $A_{\delta R}$  is set as zero. When the temperature is over 400K, the predicted curves from the modified Debye Callaway model for pure Si and for isotopic contained Si are almost the same,

which could not be discerned from Fig.3. For Pure Si,  $A_i = 0$ , and for isotopic contained  $n=0.05787\%$   $^{29}\text{Si}$ ,  $A_i = 4.259 * 10^{-48}$ . However, the two curves are collinear. So only one solid curve can be observed. The MD simulated thermal conductivities of Si with isotopic concentration of 0.05787%, i.e. there is one atom  $^{29}\text{Si}$  in  $6*6*6$  unit cell, are also plotted in Fig.3. The triangle symbol in Fig.3 stands for thermal conductivity of pure silicon evaluated from MD. Compared with the thermal conductivities of isotopic contained labeled as circle symbol, it is difficult to discern the difference of the thermal conductivity value from the MD. The difference cannot be observed yet even increasing the isotopic concentration to 0.2315%, in which there are four  $^{29}\text{Si}$  atoms in  $6*6*6$  unit cell. This agreed with the modified Debye Callaway model predictions shown as in Fig.3, in which the two predicted curves are collinear. This conclusion confirmed that at high temperature, isotopic or impurity scattering processes due to mass difference contribute little to thermal resistance.

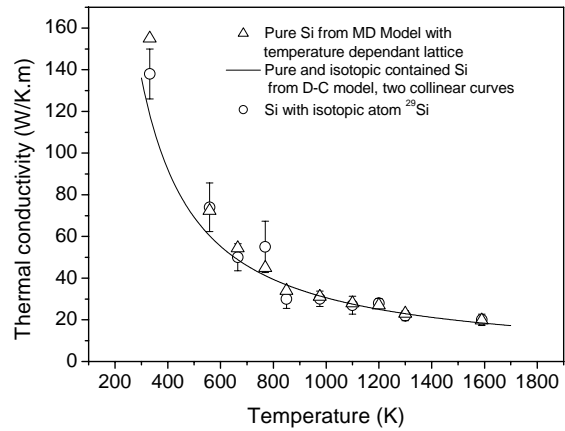


Fig.3. Isotopic effects on lattice thermal conductivity for different temperatures

Vacancies or voids may be produced during crystal growth process. In addition to the phonon being scattered due to the mass difference in isotope-phonon scattering process, the phonon may also be scattered by vacancy caused by the elastic strain in the neighbor of the voids. Formula (16) predicted that the coefficient of the vacancy-phonon scattering time due to elastic strain is about  $A_{\delta R} = 8.579 * 10^{-44}$  for  $n=0.05758\%$  vacant concentration. Compared with  $A_{\delta M} = 4.259 * 10^{-48}$ , this value  $A_{\delta R} = 8.579 * 10^{-44}$  is about four orders higher than the time coefficient of the isotope phonon scattering due to mass difference for the same  $^{29}\text{Si}$  concentrations shown in formula (13). So, the lattice thermal conductivity of crystal with void concentration will be decreased with the increase of vacancy concentration. Fig.4 explains the vacancy effects on lattice thermal conductivity very well. Compared with pure silicon case marked as solid square symbol, the case with one

vacancy in 6\*6\*6 unit cell gives smaller thermal conductivity. The error bar is also labeled in Fig.4. The maximum uncertain value of thermal conductivity is that for temperature at 800K. In order to further confirm the validity of the modified Debye Callaway model, a higher vacancy concentration simulation case is introduced. In this simulation case, two Si atoms are removed from 6\*6\*6 unit cell. The vacancy concentration is about 0.1157%. The simulated thermal conductivities for the two simulation cases are plotted in Fig.5 labeled as triangles and circles. The solid curves are evaluated from the modified Debye Callaway model. In the modified Debye Callaway model, all of the N and U scattering parameter are selected in the same value of pure silicon, which are listed in Table 3. The only varied parameter is the coefficient of impurity scattering time, which is calculated from formula (14) and (16). The simulated data agreed well with the results predicted from the modified Debye Callaway model.

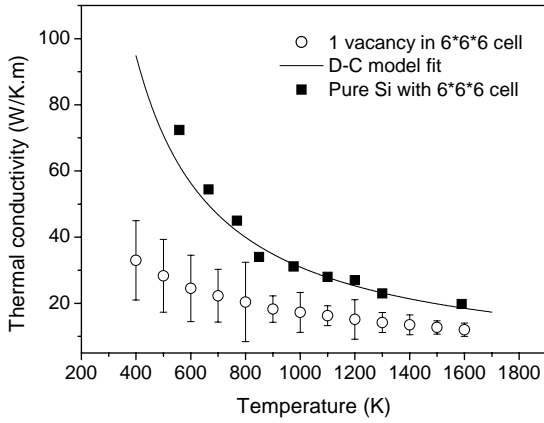


Fig.4. Lattice thermal conductivity of crystal silicon with vacancy defect

In conclusion, having computed the thermal conductivity of Si using EMD, this paper demonstrated that the trends of simulated results agreed well with the experimental data and that predicted from the modified Debye Callaway model over the temperature range from 400K to 1600K. For pure silicon, thermal expansion resulted in further decrease of the thermal conductivity with the increase of temperature. This proved that thermal expansion imposed an extra channel of thermal resistance on phonon transport besides the N and U scattering processes. Isotopic and vacancy scattering on phonons are also investigated in this MD. The MD predicted that the isotopic effects on lattice thermal conductivity can be neglected in the temperature range 400K to 1600K for defect concentration below 1%. This numerical conclusion is the same as that predicted from the modified Debye Callaway model. For vacancy defects, the mechanism of vacancy scattering on phonons includes two aspects, which refer to the scattering processes caused by mass difference and elastic strain. Compared with the same concentration of isotopic defects, the vacancy scattering on phonon is much stronger, which caused

greater decrease of lattice thermal conductivity.

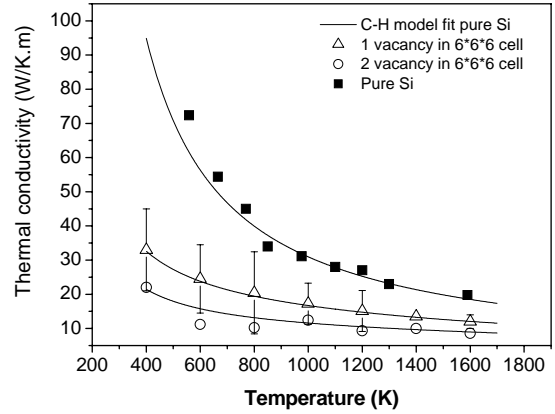


Fig.5. Lattice thermal conductivity of crystal silicon with different vacancy concentrations

Table 2 Simulation results from different simulated cell size for Si at T=800K from the fixed lattice parameter case

Atom number	Simulation time ( ns )	Thermal conductivity ( W/mK )
216	3.0	45
512	3.0	68
1000	3.0	62
1728	3.0	58

Table 3. Parameters used in this paper

Resistive process		Parameter value
Impurity scattering	$\tau_i^{-1} = (A_{\delta M} + A_{\delta R})\omega^4$	$v_s = 6.4 * 10^3$ m/s
	$A_{\delta M} = \frac{nV}{4\pi v_s^3} \left(\frac{\delta M}{M}\right)^2$	$V = 1.9 * 10^{-23} \text{ cm}^3$
	$A_{\delta R} = \frac{2nV}{\pi v_s^3} Q_0^2 \gamma^2 \left(\frac{\delta R}{R}\right)^2$	$\gamma = 0.56$
N scattering	$\tau_{TN}^{-1} = B_{TN}\omega T^4$	$B_{TN} = 7.1 * 10^{-13} \text{ s}^{-1} \text{ K}^{-5}$
	$\tau_{LN}^{-1} = B_{LN}\omega^2 T^3$	$B_{LN} = 2.4 * 10^{-24} \text{ s}^{-1} \text{ K}^{-5}$
U scattering	$\tau_{TU}^{-1} = B_{TU}\omega^2 T e^{-\theta_T/T}$	$B_{TU} = 1.0 * 10^{-19} \text{ s}^{-1} \text{ K}^{-3}, \theta_T = 240 \text{ K}$
	$\tau_{LU}^{-1} = B_{LU}\omega^2 T e^{-\theta_L/T}$	$B_{LU} = 5.50 * 10^{-20} \text{ s}^{-1} \text{ K}^{-3}, \theta_L = 586 \text{ K}$

#### Acknowledgment

The authors want to acknowledge the financial support from the National Basic Research Program of China (2006CB300404) and National Natural Science Foundation of China (50475077). This work is partly supported by the Jiangsu Province Nature Science Foundation (BK2006510) and research funding for the Doctor program from China Education Ministry (20050286019). Y. Chen also acknowledges the

financial support from the Program for New Century Excellent Talents in University (NCET-04-0470).

#### References

- [1] T.R. Anthony, W.F. Banholzer, J.F. Fleischer, L.H. Wei, P.K. Kou, R.L. Thomas, and R.W. Pryor, *Phys. Rev. B* 42, 1104, (1990).
- [2] D.G. Onn, A. Witek, Y.Z. Qiu, T.R. Anthony, W.F. Banholzer, *Phys. Rev. Lett.*, 68, 2806, (1992).
- [3] J. R. Olson, R.O. Pohl, J.W. Vandersande, A. Zoltan, T.R. Anthony, W.F. Banholzer, *Phys. Rev. B* 47, 14850, 1993.
- [4] M. Asen-Palmer, K. Bartkowski, E. Gmelin, M. Cardona, A. P. Zhernov, A. V. Inyushkin, A. Taldenkov, V. I. Ozhogin, K. M. Itoh and E. E. Haller, *Phys. Rev. B*, 56, 9431, (1997).
- [5] T. Ruffa, R.W. Henna, M. Asen-Palmera, E. Gmelina, M. Cardona, H.-J. Pohl, G.G. Devyatych, P.G. Sennikov, *Solid State Communications*, 115, 243, (2000).
- [6] T. Ruffa, R.W. Henna, M. Asen-Palmera, E. Gmelina, M. Cardona, H.-J. Pohl, G.G. Devyatych, P.G. Sennikov, *Solid State Communications*, 127, 257, (2003).
- [7] R.K. Kremera, K. Grafa, M. Cardona, G.G. Devyatych, A.V. Gusevb, A.M. Gibinb, A.V. Inyushkinc, A.N. Taldenkov, H.-J. Pohl, *Solid State Communications*, 131, 499, (2004).
- [8] A.V. Inyushkin, *Inorg. Mater.* 18, 427(2002).
- [9] D. T. Morelli and J. P. Heremans, G. A. Slack, *Phys. Rev. B*, 66, 195304, (2002).
- [10] P.G. Klemens, in *Solid State Physics*, edited by F. Seitz and D. Turnbull (Academic, New York, 1958), Vol. 7, P.59.
- [11] J. Callaway, *Phys. Rev.* 113, 1046 (1959).
- [12] M.G. Holland, *Phys. Rev.* 132, 246 (1963).
- [13] A. Sparavigna, *Phys. Rev. B*, 65, 064305 (2002).
- [14] J.W. Bray and T.R. Anthony, *Z. Phys. B* 84, 51 (1991).
- [15] K. C. Hass, M. A. Tamor, T. R. Anthony, and W. F. Banholzer, *Phys. Rev. B* 45, 7171 (1992).
- [16] A. Murakawa, H. Ishii, K. Kakimoto, *Jour. of Crystal Growth* 267, 452–457, (2004).
- [17] F. Clayton and D. N. Batchelder, *J. Phys. C* 6, 1213 (1973).
- [18] D. K. Christen and G. L. Pollack, *Phys. Rev. B* 12, 3380 (1975).
- [19] C.J. Glassbenner, G.A. Slack, *Phys. Rev.* 134, A1058, (1961).
- [20] J. S. Dugdale and D. K. MacDonald, *Phys. Rev.* 98, 1751 (1955).
- [21] Volz S G, Chen G. *Phys. Rev. B*, 61, 2651, (2000).
- [22] Li J, Porter L, Yip S. *Jour. of Nuclear Mater.*, 255:139-152 (1998).
- [23] Y.H. Lee, R. Biswas, C.M. Soukoulis, C.Z. Wang, C.T. Chan and K.M. Ho, *Phys. Rev. B*, 43, 6573, (1991).
- [24] C. Oligschleger, J. C. Schon, *Phys. Rev. B*, 59, 4125 (1999).
- [25] P.K. Schelling, S.R. Phillpot, P. Keblinski, *Phys. Rev. B*, 65, 144306, (2002).
- [26] F.H. Stillinger, T.A. Weber, *Phys. Rev. B*, 31, 5262, (1985).
- [27] M. Asheghi, K. Kurabayashi, R. Kasavi, and K. E. Goodson, *J. Appl. Phys.* 91, 5079, (2002).

[28] J.R. Lukes, D.Y. Li, X.G. Li and C.L. Tien, *Journal of Heat Transfer*, 116(3), 536-543, 2000.